

Scanning plasmon near-field microscopy: signal–noise ratio of different registration schemes and prospects for single molecule detection†

V. N. Konopsky,^{*a} S. A. Saunin,^b V. A. Bykov^b and E. A. Vinogradov^a

^a *Institute of Spectroscopy, Russian Academy of Sciences, Troitsk, Moscow region, 142190, Russia*

^b *NT-MDT Co., State Research Institute of Physical Problems, Zelenograd, Moscow, 103482, Russia*

Received 1st November 2001, Accepted 25th March 2002

First published as an Advance Article on the web 13th May 2002

Possible registration schemes of scanning plasmon near-field microscopes (SPNMs) are considered and their signal–noise ratios are evaluated. A comparison among these schemes is made with particular attention to the best scheme for a single molecule detection by a SPNM.

1 Introduction

Apertureless version of a scanning near-field optical microscope (SNOM) has attracted considerable attention in recent years. It is because of its simplicity, high power of an optical signal and highest spatial near-field resolution that such apertureless scanning near-field optical microscopes (aSNOMs) are demonstrated in comparison with standard SNOMs. One of the most interesting feature of aSNOMs is the possibility of localization and enhancement of the electromagnetic (em) field near the tip. Such increasing of the em field is especially strong if the tip is coated by (or consists of) a noble metal and may be used to enhance the fluorescence of dye molecules near the apertureless probe.^{1–3} The enhancement of the em field at the tip appears to be particularly promising for detecting nonlinear optical effects such as two-photon excitation of the fluorescence⁴ or enhanced Raman scattering^{5–7} of the molecules near the probe.

In recent papers^{8,9} it was shown that one can reach near-field resolution of even less than tip radius (and obtain huge field enhancement) using the em resonance in the noble metal tip–noble metal surface structure. This resonance manifests itself as an extremum in detected light intensity during the tip approach toward (and withdrawal from) the surface. Such extrema in the distance-dependent light signal intensity were detected not only in SPNMs,^{10–12} but also in other modification of SNOMs where the tip and surface were coated with noble metals.^{13,14} In the work⁸ these extrema were interpreted as an em resonance in the tip–surface structure and it was proposed to record the light signal at the second harmonic of a tapping frequency to pick out the signal associated with this resonance. Inasmuch as the spacing between the tip and the surface at which the em resonance occurs is depended on intermediate medium permittivity ($d_{\text{res}} \sim \epsilon_0^2$), study of the local permittivities with subtip resolution is possible.⁹ For example, molecules with a resonance line near the laser frequency deposited on the surface may be visualized in such a manner (in Section 4 we describe this approach in detail).

The prospects for single molecule detection by SPNM makes it important to estimate the signal–noise ratio of different registration modes of SPNM. The present work is devoted to this problem.

2 Registration modes of SPNM

The principle of the SPNM scheme in the usual Kretschmann configuration is shown in Fig. 1. A beam of a laser incident on a silver film (with thickness ~ 50 nm), at a defined angle θ_0 of total internal reflection, excites the surface plasmons at the silver–air interface.

Several registration modes of the light signal may be used in SPNMs:

(1) “Internal reflection” registration mode—registration of the intensity variation of the reflected light beam by photodiode N1.

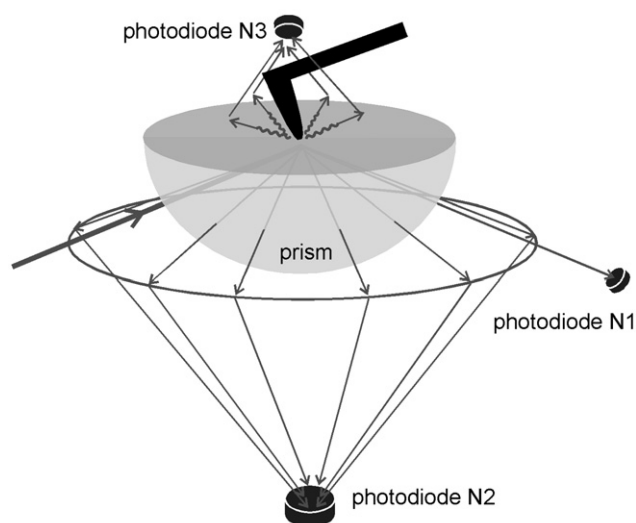


Fig. 1 A principal scheme of the scanning plasmon near-field microscope.

† Presented at the LANMAT 2001 Conference on the Interaction of Laser Radiation with Matter at Nanoscopic Scales: From Single Molecule Spectroscopy to Materials Processing, Venice, 3–6 October, 2001.

(2) “Internal scattering” registration mode—registration of the intensity of the conical light radiation (arisen from an elastic scattering of the surface plasmons) by photodiode N2 (conical scattered light radiation is collected by a cylindrical mirror).

(3) “External scattering” registration mode—registration of the plasmon–photon scattering by photodiode N3.

In ref. 11 the authors claimed that the “internal scattering” registration mode is more sensitive than “internal reflection” registration mode which was used in the first SPNM work.¹⁰ Below we show that the signal–noise ratio of these schemes is dependent on many factors such as the roughness of the silver film, the radius of the tip, the laser frequency and so on. In particular, at small tip radii the “internal reflection” registration mode becomes more sensitive than others.

3 Signal–noise ratio of the registration modes

3.1 “Internal reflection” registration mode

The light beam incident on the photodiode N1 induces a current

$$i_1 = \eta e I_0 r, \quad (1)$$

where e is the electron charge, I_0 is the initial laser power [photons s^{-1}], r is the internal reflection coefficient of the silver film on quartz at plasmon resonance (*i.e.* at the minimum of reflection; at best $r \sim 0.01 \dots 0.1$) and η is the photodetector quantum efficiency.

This current has a noise spectral density which may be found by the Schottky formula

$$\sqrt{\langle (\delta i_1)^2 \rangle} = \sqrt{2e i_1 \Delta f}, \quad (2)$$

where $\Delta f = (2t_m)^{-1}$ is the bandwidth of the measurement, t_m is the measurement time.

The useful change of the signal at photodiode N1 induced by the tip is

$$\Delta i_1 \simeq \eta e \frac{I_0}{\pi \rho^2} S_{\text{tip}}^{\text{total}}, \quad (3)$$

where ρ is a radius of the light beam at the surface beneath the tip, $S_{\text{tip}}^{\text{total}}$ is the cross-section of the total losses in the plasmon beam induced by the tip–surface structure. This total cross-section is consisted from several parts:

$$S_{\text{tip}}^{\text{total}} = S_{\text{tip}}^{\text{pl-pl}} + S_{\text{tip}}^{\text{pl-ph}} + S_{\text{tip}}^{\text{abs}}, \quad (4)$$

where $S_{\text{tip}}^{\text{pl-pl}}$ is the cross-section of the scattering of SPs from the initial plasmon beam to other plasmon states (with different propagation directions), $S_{\text{tip}}^{\text{pl-ph}}$ is the cross-section of the scattering of SPs to photons and $S_{\text{tip}}^{\text{abs}}$ is the cross-section of the absorption of SPs by the tip–surface structure.

In the registration mode under consideration the signal–noise ratio is

$$\frac{\text{Signal}}{\text{Noise}} = \frac{\Delta i_1}{\sqrt{\langle (\delta i_1)^2 \rangle}} \simeq \sqrt{\frac{\eta I_0 t_m}{r}} \frac{S_{\text{tip}}^{\text{total}}}{\pi \rho^2}. \quad (5)$$

3.2 “Internal scattering” registration mode

The light beam collected by the cylindrical mirror on the photodiode N2 induces the current

$$i_2 \simeq \eta e \frac{I_0}{\pi \rho^2} S_{\text{unit}}^{\text{pl-pl}} = \eta e I_0 S_{\text{unit}}^{\text{pl-pl}}, \quad (6)$$

where $S_{\text{unit}}^{\text{pl-pl}}$ is the total plasmon–plasmon scattering cross section from the illuminated area $\pi \rho^2$ caused by surface roughness (without a tip). Since this total cross-section is linearly proportional to the illuminated area, we introduce a dimensionless

(normalized to the the illuminated area) quantity $S_{\text{unit}}^{\text{pl-pl}} \equiv S_{\text{unit}}^{\text{pl-pl}} / \pi \rho^2$, which is the cross-section of the roughness-induced plasmon–plasmon scattering from a unit surface area.

The useful change of the signal at photodiode N2 induced by the tip is

$$\Delta i_2 \simeq \eta e \frac{I_0}{\pi \rho^2} S_{\text{tip}}^{\text{pl-pl}}. \quad (7)$$

In this registration mode the signal–noise ratio is

$$\frac{\text{Signal}}{\text{Noise}} = \frac{\Delta i_2}{\sqrt{\langle (\delta i_2)^2 \rangle}} \simeq \sqrt{\frac{\eta I_0 t_m}{S_{\text{unit}}^{\text{pl-pl}}}} \frac{S_{\text{tip}}^{\text{pl-pl}}}{\pi \rho^2}. \quad (8)$$

To estimate the quantity $S_{\text{unit}}^{\text{pl-pl}}$ we will use formula for a SP attenuation length associated with roughness-induced SP scattering into other SP states:

$$L_{\text{pl-pl}} = \frac{2}{3} \left(\frac{c}{\omega} \right)^5 \frac{|\epsilon'|}{\sigma^2 \delta^2}, \quad (9)$$

which was obtained by Mills¹⁵ (see also ref. 16). Here σ is the transverse correlation length of the surface roughness, δ is the root-mean square of the surface roughness and $\epsilon = \epsilon' + i\epsilon''$ is the dielectric constant of the surface.

For a typical thermally evaporated silver film on quartz substrate, $\delta \simeq 1.5$ nm; $\sigma \simeq 200$ nm; $\epsilon' \simeq -18$ (for $\lambda \simeq 632$ nm). In this case $L_{\text{pl-pl}} (\simeq 1060 \mu\text{m})$. Thereafter we will use these values for numerical examples (in brackets). Other numerical values that will be used for examples are: $\epsilon'' \simeq 0.5$ (for $\lambda \simeq 632$ nm); $\eta \simeq 0.1$; $I_0 \simeq 10$ mW $\simeq 3 \times 10^{16}$ photons s^{-1} ; $t \simeq 0.01$ s; $\pi \rho^2 \simeq 100 \times 100 \mu\text{m}^2$.

A SP attenuation length associated with roughness-induced SP scattering into the vacuum^{15,16} will be used below:

$$L_{\text{pl-ph}} = \frac{3}{4} \left(\frac{c}{\omega} \right)^5 \frac{|\epsilon'|^{1/2}}{\sigma^2 \delta^2} (\simeq 280 \mu\text{m}). \quad (10)$$

These relations are valid for $|\epsilon'| \gg 1$, and for surfaces with the transverse correlation length σ less than the SP wavelength.

It is known that in most cases the mean free path of SPs L_{sp} is determined by internal absorption of the SP energy in the metal, and therefore

$$\frac{1}{L_{\text{sp}}} = \frac{1}{L_{\text{pl-pl}}} + \frac{1}{L_{\text{pl-ph}}} + \frac{1}{L_{\text{abs}}} \approx \frac{1}{L_{\text{abs}}} \quad (11)$$

where L_{abs} is¹⁶

$$L_{\text{abs}} = \frac{c}{\omega} \frac{|\epsilon'|^2}{\epsilon''} \left(\frac{\epsilon' + 1}{\epsilon'} \right)^{3/2} \approx \frac{c}{\omega} \frac{|\epsilon'|^2}{\epsilon''}. \quad (12)$$

Substituting above given values into eqn. (12) one can obtain $L_{\text{abs}} \simeq 62 \mu\text{m}$. But in Kretschmann configuration, at optimal film thickness, a real plasmon free path is halved due to leakage of the energy in prism side.¹⁶ Therefore $L_{\text{sp(Kret)}} \simeq 31 \mu\text{m}$.

To obtain the estimation for $S_{\text{unit}}^{\text{pl-pl}}$ in the case under consideration ($L_{\text{sp}} \sim L_{\text{abs}} \ll L_{\text{pl-pl}}, L_{\text{pl-ph}}$), we note that value of the scattering radiation is

$$I_2 = I_0 S_{\text{unit}}^{\text{pl-pl}} \simeq I_0 \frac{L_{\text{sp}}}{L_{\text{pl-pl}}} \quad (13)$$

Therefore, in Kretschmann configuration

$$S_{\text{unit}}^{\text{pl-pl}} \approx \frac{L_{\text{sp(Kret)}}}{L_{\text{pl-pl}}} \simeq \frac{3}{4} \left(\frac{\omega}{c} \right)^4 \frac{|\epsilon'|}{\epsilon''} \sigma^2 \delta^2 (\simeq 1/34). \quad (14)$$

3.3 “External scattering” registration mode

The current of the photodiode N3 induced by photons (arising from plasmon–photon scattering by surface roughness) is

$$i_3 \simeq \eta e \frac{I_0}{\pi \rho^2} S_{\text{unit}}^{\text{pl-ph}} = \eta e I_0 S_{\text{unit}}^{\text{pl-ph}}, \quad (15)$$

where $S_{\pi\rho^2}^{\text{pl-ph}}$ is the total cross-section of roughness-induced plasmon–photon scattering from the illuminated area $\pi\rho^2$, $S_{\text{unit}}^{\text{pl-ph}}$ is the cross-section of plasmon–photon scattering from a unit surface. The efficiency of the collecting optics is included in the quantity η .

The useful change of the signal at photodiode N3 induced by the tip is

$$\Delta i_3 \simeq \eta e \frac{I_0}{\pi\rho^2} S_{\text{tip}}^{\text{pl-ph}}. \quad (16)$$

The signal–noise ratio of this registration mode is

$$\frac{\text{Signal}}{\text{Noise}} = \frac{\Delta i_3}{\sqrt{\langle (\delta i_3)^2 \rangle}} \simeq \sqrt{\frac{\eta I_0 t_m}{S_{\text{unit}}^{\text{pl-ph}} \pi\rho^2}} S_{\text{tip}}^{\text{pl-ph}}. \quad (17)$$

The quantity $S_{\text{unit}}^{\text{pl-ph}}$ is

$$S_{\text{unit}}^{\text{pl-ph}} \approx \frac{L_{\text{sp}}(\text{Kret})}{L_{\text{pl-ph}}} \simeq \frac{2}{3} \left(\frac{\omega}{c} \right)^4 \frac{|\epsilon'|^{3/2}}{\epsilon''} \sigma^2 \delta^2 (\simeq 1/9). \quad (18)$$

And, as a numerical example for the values given above, one can see that $S_{\text{tip}}^{\text{pl-ph}}$ must be about $\sim 80 \times 80 \text{ nm}^2$, to obtain a S/N ratio of about 10. It should be mentioned that, at em resonance, the scattering (and absorption) cross-sections of the tip–surface structure may be larger than the geometrical size of the tip. For the same numerical values $S_{\text{tip}}^{\text{pl-ph}}$ must be about $\sim 56 \times 56 \text{ nm}^2$, to obtain a S/N ratio of about 10.

Here it may be noted that in some cases (for example, at registration of nonlinear effects such as second harmonic generation or Raman scattering) the noise signal will be determined by the dark current of a photodetector i_{dark} . In these cases (at $i_3 < i_{\text{dark}}$) the signal–noise ratio may be written in the next form:

$$\frac{\text{Signal}}{\text{Noise}} = \frac{\Delta i}{\sqrt{\langle (\delta i_{\text{dark}})^2 \rangle}} \simeq \sqrt{\frac{e t_m}{i_{\text{dark}}}} \eta I_0 \frac{S_{\text{tip}}^{\text{nonlin}}(I_0)}{\pi\rho^2}. \quad (19)$$

4 Prospects for single molecule detection by SPNM

In this section we describe in more detail possible employment of the tip–surface em resonance for single molecule detection to explain why the choice of the registration method with the best S/N ratio is important.

In the work⁹ it was pointed out that a SPNM may be used for visualization of a single molecule on a surface by registration of the *spacing* between the tip and the surface at which the em resonance occurs. This spacing is:^{8,9}

$$d_{\text{res}} = 2R \left[\frac{\epsilon'_0(\omega)}{|\epsilon'_1(\omega)|} + \frac{\epsilon'_0(\omega)}{|\epsilon'_2(\omega)|} \right]^2, \quad (20)$$

where $\epsilon'_2(\omega)$ and $\epsilon'_1(\omega)$ are the real parts of the permittivities of a tip and a surface, R is a radius of curvature of the tip and $\epsilon'_0(\omega)$ is a real part of the permittivity of an intermediate medium between the tip and the surface. Hence the detection of the d_{res} (at each point of the surface) may give the information about the permittivities of the intermediate medium ($\epsilon'_0(\omega)$ at each surface point) with resolution.^{8,9}

$$L \approx \sqrt{2d_{\text{res}}R} \approx 2R \left[\frac{\epsilon'_0(\omega)}{|\epsilon'_1(\omega)|} + \frac{\epsilon'_0(\omega)}{|\epsilon'_2(\omega)|} \right] < R. \quad (21)$$

If the molecule to be detected has an absorption band at the frequency ω_{mol} (see Fig. 2) then tuning the laser frequency at ω_- (or below), where $\epsilon'_0(\omega)$ has the maximum (or near the maximum), one can reveal the molecule location by detecting the change of d_{res} .

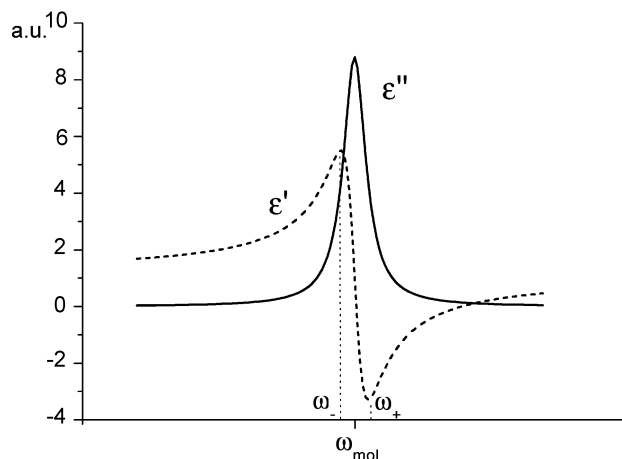


Fig. 2 Permittivities $\epsilon'(\omega)$ and $\epsilon''(\omega)$ of the volume $L^2 d_{\text{res}}$ between the tip and the surface, near molecular resonance line.

The permittivity of the intermediate medium (without the resonance molecule) is

$$\epsilon_{0(\text{w.mol.})} = 1 + \frac{4\pi N f_{\text{env}} e^2 / m}{\omega_{\text{env}}^2 - \omega^2 + 2i\omega\gamma_{\text{env}}} \quad (22)$$

where ω_{env} is the resonance frequency of the intermediate medium (e.g. air), γ_{env} and f_{env} the damping constant and oscillator strength of this resonance and N is the number of molecules in the unit volume. When the environment is the air, $\epsilon_{0(\text{w.mol.})}$ is only a trifle over unity ($\epsilon_{\text{air}} \simeq 1.0003$).

The presence of the resonance molecule in the measured volume $L^2 d_{\text{res}}$ leads to an additional term in the permittivity equation:

$$\epsilon_0 = \epsilon_{0(\text{w.mol.})} + \frac{4\pi f_{\text{mol}} e^2 / m}{\omega_{\text{mol}}^2 - \omega^2 + 2i\omega\gamma_{\text{mol}}} \frac{1}{L^2 d_{\text{res}}} \quad (23)$$

From eqn. (23) one can see that the smaller the em field localization L the easier it is to detect the change in ϵ'_0 .

So, in this method one can detect a single molecule on the surface not by registration of a (weak) signal of a scattering or absorption induced by a single molecule, but by detecting a change of dielectric permittivity in the small volume $L^2 d_{\text{res}}$ induced by the single molecule through registration of a (strong) signal of a SPNM registration mode. The described method has the same advantages as all *phase* methods (e.g. insensitivity to intensity), since one detects the position of the em extremum d_{res} , but not the extremum amplitude (which depends on the em intensity). Therefore noise, associated with laser intensity and with plasmon field distribution on the surface should be strongly suppressed.

We assume that the main interference for detection of a useful signal (associated with change of local permittivity induced by a single molecule) will be the change of d_{res} associated with local surface roughness under tip. Indeed, in eqn. (20) R is the relative curvature $(1/R_{\text{tip}} + 1/R_{\text{surface}})^{-1}$, where R_{surface} is the local curvature of the surface at the point of the observation ($R_{\text{surface}} = \infty$ at the flat surface). To avoid this type of noise one can use the second laser adjusted on the frequency ω_+ (see Fig. 2) and subtract two values: $d_{\text{res}}(\omega_-) - d_{\text{res}}(\omega_+)$. Under this approach the useful signals will be doubled, but roughness-induced interference signals will be suppressed.

Last, but not least, the advantage of the described single molecule detection method is possibility of decreasing photo-bleaching of the molecule under study by detuning the exciting light frequencies ω_- and ω_+ as far from the resonance frequency ω_{mol} as possible.

Obviously, the better S/N ratio of a registration mode the easier it is to detect small changes in d_{res} .

5 Discussion

Now let us compare the signal–noise ratio of the “internal scattering” [eqn. (8)] and “external scattering” [eqn. (17)] registration modes. For these purposes we must compare the values $s_{\text{unit}}^{\text{pl-pl}}$ and $s_{\text{unit}}^{\text{pl-ph}}$. As it was shown by Mills,¹⁵ on the basis of a numerical evaluation of full formulas for $L_{\text{pl-pl}}$ and $L_{\text{pl-ph}}$, the radiation loss (plasmon–photon scattering) is more effective than the plasmon–plasmon scattering at

$$|\varepsilon'| \geq 7 \quad (24)$$

i.e., at longer wavelength. This is due to similarity of SPs and photons in this region (a SP dispersion curve and a light line are close together in this case). For $|\varepsilon'| \rightarrow 1$ the reverse holds: the value $s_{\text{unit}}^{\text{pl-pl}}$ becomes larger than $s_{\text{unit}}^{\text{pl-ph}}$.

It would appear reasonable that the values $S_{\text{tip}}^{\text{pl-pl}}$ and $S_{\text{tip}}^{\text{pl-ph}}$ change in an analogous way (*i.e.*, we consider the tip as “artificial roughness”). We will make this assumption since there are no simple formulas available for cross-sections of the tip–surface structure ($S_{\text{tip}}^{\text{pl-pl}}$, $S_{\text{tip}}^{\text{pl-ph}}$ and $S_{\text{tip}}^{\text{abs}}$). It may be noted here that the dipole approximation, which sometimes is used^{10,17,18} in this area of research, is inappropriate for this purpose (at least in the case of metal surfaces). The dipole approximation is the consideration of the tip–surface (*i.e.* sphere–plane) structure as a dipole together with its mirror image in a sample. This model may be used only at large distances between the tip and the surface. However at small distances (smaller than the tip radius) the contribution of higher order sphere multiples becomes significant and the dipole approximation yields incorrect results. The comparison between the dipole approximation and the exact calculation for dielectric and metal surfaces was made in ref. 19. Furthermore, the dipole approximation predicts no extrema on the light signal approach curve, but such extrema experimentally detected at appropriate conditions.^{8,10–14} The model taking into account the em tip–surface resonance seems to be more adequate for the SPNM experimental conditions.⁸

Most of the SPNM experiments are performed in the wavelength region where inequality (24) is fulfilled. In this case roughness-induced plasmon–photon scattering is larger than roughness-induced plasmon–plasmon scattering (*i.e.* $s_{\text{unit}}^{\text{pl-ph}} > s_{\text{unit}}^{\text{pl-pl}}$) and the noise signal is larger in the “external scattering” mode. But according to our assumption $S_{\text{tip}}^{\text{pl-ph}}$ should be also larger than $S_{\text{tip}}^{\text{pl-pl}}$. Since these signal–noise ratios are linear in S_{tip} and inversely proportional to the square root of s_{unit} , the “external scattering” mode is more sensitive in this frequency region. The possible “antenna effect” of the needle should also increase the useful signal in “external scattering” registration mode. Certainly, it is more difficult to collect uniformly the total light signal in the “external scattering” scheme. It is material practical disadvantage of this scheme since the nonuniformity in the registration of the scattered light leads to certain artifacts in near-field images.⁹

Now we compare the signal–noise ratio of the “internal reflection” registration scheme and “scattering” registration schemes. A comparison between eqns. (5), (8) and (17) show that on very flat surfaces ($\delta \rightarrow 0$) the “scattering” registration schemes would be very sensitive. However according to eqn. (4) the cross-section of the tip-induced losses in the plasmon beam ($S_{\text{tip}}^{\text{total}}$) is always greater than the scattering cross-sections, at least by the value of $S_{\text{tip}}^{\text{abs}}$. As noted above the cross-sections of the light scattering and absorption by the tip–surface structure obtained in the dipole approximation may be used only at large distances between the tip and the surface. But we assume that some *qualitative* characteristics

of these cross-sections may be used for qualitative estimations. Under the dipole approximation

$$S_{\text{tip}}^{\text{abs}} \sim R^3/\lambda, \quad (25)$$

where λ is the wavelength and R is the radius of the tip, while the scattering cross-sections

$$S_{\text{tip}}^{\text{sc}} \sim R^6/\lambda^4. \quad (26)$$

That is, at $R \rightarrow 0$ the value $S_{\text{tip}}^{\text{sc}}$ becomes much less than $S_{\text{tip}}^{\text{total}} (\geq S_{\text{tip}}^{\text{abs}})$. Furthermore, for ultrasharp tips (at $R \sim \lambda v_F/c$, where v_F is the Fermi’s velocity of electrons in the metal), the process of generation of electron–hole pairs by the short-wavelength Fourier components of the em field becomes the strongest damping mechanism in the system. Therefore it is impossible to reach the best sensitivity in “scattering” schemes (at least on surfaces with ordinary roughness) if one also wants to obtain an ultimate spatial resolution (*i.e.* must to work with ultrasharp tips).

6 Conclusions

From consideration of the signal–noise ratios of different registration modes presented here these conclusions may be made:

- (1) To obtain the best resolution in “scattering” schemes an ultraflat ($\delta \rightarrow 0$) metal film must be used.
- (2) At ($|\varepsilon'| \rightarrow 1$) the “internal scattering” registration mode has better sensitivity than the “external scattering” registration mode.
- (3) At longer wavelengths ($|\varepsilon'| \geq 7$) the reverse holds: the “external scattering” registration mode has the better sensitivity than the “internal scattering” mode, subject to a good light collecting scheme in this mode.
- (4) At ultimate spatial resolution (*i.e.* at $R \rightarrow 0$) the “internal reflection” registration mode has the best sensitivity in comparison to “scattering” modes on surfaces with ordinary roughness.
- (5) In all schemes tight focussing of the light beam beneath the tip (as tight as possible from experimental conditions) is required to reach the best signal–noise ratio.

Acknowledgement

The present research was supported by the Russian Foundation for Basic Research and Ministry of Industry, Science and Technology of the Russian Federation. One of the authors (V. N. Konopsky) thanks INTAS for Young Scientists grant YSF 2001/1-106.

References

- 1 J. Azoulay, A. Débarre, A. Richard and P. Tchéno, *J. Microsc. (Oxford)*, 1999, **194**(2–3), 486.
- 2 H. F. Hamman, A. Gallagher and D. J. Nesbitt, *Appl. Phys. Lett.*, 1998, **73**(11), 1469.
- 3 H. F. Hamman, A. Gallagher and D. J. Nesbitt, *Appl. Phys. Lett.*, 2000, **76**(14), 1953.
- 4 E. J. Sánchez, L. Novotny and X. S. Xie, *Phys. Rev. Lett.*, 1999, **82**(20), 4014.
- 5 R. M. Stöckle, Y. D. Suh, V. Deckert and R. Zenobi, *Chem. Phys. Lett.*, 2000, **318**(1–3), 131.
- 6 N. Hayazawa, Y. Inouye, Z. Sekkat and S. Kawata, *Opt. Commun.*, 2000, **183**(1–4), 333.
- 7 L. T. Nieman, G. M. Krampert and R. E. Martinez, *Rev. Sci. Instrum.*, 2001, **72**(3), 1691.
- 8 V. N. Konopsky, *Opt. Commun.*, 2000, **185**(1–3), 83.
- 9 V. N. Konopsky, K. E. Kouyanov and N. N. Novikova, *Ultramicroscopy*, 2001, **88**(2), 127.

- 10 M. Specht, J. D. Pedarnig, W. M. Heckl and T. W. Hänsch, *Phys. Rev. Lett.*, 1992, **68**, 476.
- 11 Y.-K. Kim, P. M. Lundqvist, J. A. Helfrich, J. M. Mikrut, G. K. Wong, P. R. Auil and J. B. Ketterson, *Appl. Phys. Lett.*, 1995, **66**, 3407.
- 12 J. Boneberg, M. Ochmann, H.-J. Münzer and P. Leiderer, *Ultra-microscopy*, 1998, **71**, 345.
- 13 U. Ch. Fischer and D. W. Pohl, *Phys. Rev. Lett.*, 1989, **62**(4), 458.
- 14 J. Ferber, U. Ch. Fischer, N. Hagedorn and H. Fuchs, *Appl. Phys. A*, 1999, **9**, 581.
- 15 D. L. Mills, *Phys. Rev. B*, 1975, **12**(10), 4036.
- 16 H. Raether, *Surface Plasmons*, Springer-Verlag, Berlin, 1988, vol. 111, p. 36.
- 17 B. Knoll and F. Keilmann, *Nature*, 1999, **399**, 134.
- 18 B. Knoll and F. Keilmann, *Opt. Commun.*, 2000, **182**, 321.
- 19 R. Ruppin, *Surf. Sci.*, 1983, **127**, 108.